Calcium-Triggered Selective Intermembrane Exchange of Phospholipids by the Lung Surfactant Protein SP-A†

Yolanda Cajal,‡,§ Chandra Dodia,|| Aron B. Fisher,|| and Mahendra K. Jain*,‡

Department of Chemistry and Biochemistry, University of Delaware, Newark, Delaware 19716, Institute for Environmental Medicine, University of Pennsylvania School of Medicine, Philadelphia, Pennsylvania 19104, and Facultat de Farmacia, Unitat de Fisicoquimica, University of Barcelona, 08028 Spain

Received January 16, 1998; Revised Manuscript Received May 15, 1998

ABSTRACT: It is shown that human lung surfactant protein (SP-A) mediates selective exchange of phospholipid probes with unlabeled phospholipid in excess vesicles in the presence of calcium and NaCl. The exchange occurs without leakage of vesicle contents, or transbilayer movement (flip-flop) of the phospholipid probes, or fusion of vesicles. Individual steps preceding the exchange are dissected by a combination of protocols, and the results are operationally interpreted in terms of a model where a calcium-dependent change in SP-A triggers aggregation of vesicles followed by probe exchange between the vesicles in contact through SP-A. The contacts remain stable in the presence of calcium; i.e., the vesicles in contact do not change their partners on the time scale of several minutes. The binding of SP-A to vesicles and the aggregation of vesicles are rapid, and the aggregation is rapidly reversed by EGTA; i.e., both the forward and reverse aggregation reactions are complete in about 1 min. The exchange rate of the various probes between aggregated vesicles below 1 mM calcium in the presence of NaCl shows selectivity, i.e., a modest dependence on the net anionic charge on vesicles and for the headgroup of the probe. Exchange with lower selectivity is seen at >2 mM Ca in the absence of NaCl. SP-A binding to vesicles does not show an absolute specificity for the phospholipid structure, but the time course of the subsequent changes does. The results suggest that SP-A contacts between phospholipid interfaces could mediate the exchange of phospholipid species (trafficking and sorting) between lung surfactant pools in the hypophase and all accessible phospholipid interfaces of the alveolar space.

Lung surfactant protein A (SP-A),[1] along with two other surfactant-specific proteins (B and C), constitute the bulk of proteins that co-isolate with the lung surfactant (1−3). Interaction of these proteins with phospholipid regulates the surface properties of the surfactant, which makes breathing an imperceptible effort at a frequency of >20 000 cycles per day. SP-A, a hydrophilic protein, exists in the alveolar space as an octadecameric aggregate (*4*, *5*) of a variably glycosylated monomer (29−36 kDa) of a primary sequence of 263 residues (26 kDa) with a collagen like segment and a carbohydrate recognition region specific for mannose and galactose (*2*). SP-A binds calcium (*6*) and to phosphatidylcholines (*7*, *8*), as demonstrated by electron microscopy (*9*), thin-layer chromatography (*10*), aggregation (*11*−*13*), intrinsic tryptophan fluorescence methods (*14*), and mutagenesis (*15*). A preference for DPPC, the major phospholipid component of lung surfactant, which appears to be primarily responsible for its biological activity at interfaces, was noted in some of these studies. The physiological role for the interaction of SP-A with phospholipid remains to be established; however, SP-A has been implicated in regulation of phospholipid secretion and uptake (*13*, *16*), lowering of phospholipase A_2 activity (*11*), generation of tubular myelin (*17*), formation of a stable phospholipid monolayer (*2*), and modulation of the gel−fluid phase properties of the bilayer (*7*). It also appears that the phospholipid composition, pH, salt and calcium concentrations, and galactose and mannose lectin properties of SP-A contribute to its overall function (*1*−*3*).

We show that a calcium-induced change in SP-A mediates a direct, rapid, and selective exchange of phospholipid between vesicles without fusion or solubilization. The exchange is characterized by adopting some of the remarkably sensitive methods developed during the past decade for detection of bilayer apposition, lipid exchange, mixing, and fusion (*18*−*22*). These probe-based methods have proven quite useful for demonstrating the selectivity of the phos-

† This work was supported by the NIH (Grants GM29703 to M.K.J. and HL19737 to A.B.F.).

* To whom correspondence should be addressed.
‡ University of Delaware.
§ University of Barcelona.
|| University of Pennsylvania School of Medicine.

[1] Abbreviations: ANTS, 1-aminonaphthalene-3,6,8-trisulfonic acid; DMPG, 1,2-dimyristoylglycero-*sn*-3-phosphoglycerol; DMPM, 1,2-dimyristoylglycero-*sn*-3-phosphomethanol; DNS-PE, *N*-dansylphosphatidylethanolamine (egg); DPPC, 1,2-dipalmitoylphosphatidylcholine; DTGPE-DNS, N-dansylated 1,2-ditetradecylglycero-*sn*-3-phosphoethanolamine; DPX, *N*,*N*′-*p*-xylenebis(pyridinium bromide); DTPM, 1,2-ditetradecylglycero-*sn*-3-phosphomethanol; HDNS, *N*-dansylhexadecyl-1-phosphoethanolamine; NBD-PE, *N*-(7-nitro-2,1,3-benzoxadiazol-4-yl)dioleoylphosphatidylethanolamine; POPC, 1-palmitoyl-2-oleoylglycero-*sn*-3-phosphocholine; POPG, 1-palmitoyl-2-oleoylglycero-*sn*-3-phosphoglycerol; PyPX, 1-hexadecanoyl-2-(1-pyrenedecanoyl)glycero-*sn*-3-phospho-X (X = C, choline; G, glycerol); PySM, pyrene-labeled sphingomyelin; R18, octadecyl rhodamine; RET, resonance energy transfer; Rh-PE, *N*-(lissamine rhodamine B sulfonyl)dioleoyl phosphatidylethanolamine; SP-A, human lung surfactant protein A.

S0006-2960(98)00122-6 CCC: $15.00
Published on Web 08/12/1998

Scheme 1: Equilibrium Relationship between the SP-A Species That Participate in Various Reactions Described in the Text

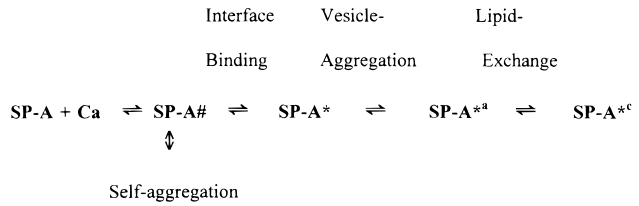

pholipid exchange mediated by polymyxin B (*23*−*25*), mellitin (*26*), and myelin basic protein (*27*). In this paper, we show that intervesicle contacts formed by a few molecules of SP-A per vesicle mediate selective exchange of phospholipid through the vesicle−vesicle contacts.

To facilitate the presentation of results and the discussion, we adopt a heuristic model that has been useful in earlier studies on peptide and protein-mediated phospholipid exchange. Operationally, as outlined in Scheme 1, sequential steps relating five functionally different SP-A species are distinguishable. Calcium changes SP-A in the aqueous phase to SP-A#, which binds to phospholipid vesicles. Three membrane-bound species are marked with an asterisk. Following the initial binding, the bound SP-A* promotes aggregation of vesicles, presumably by changing to the SP-A*^{a} form. The lipid exchange between the aggregated vesicles is seen only under certain conditions, which suggests that the exchange is mediated by yet another species, SP-A*^{c}, that forms a functional contact between two vesicles. NaCl promotes the calcium-mediated formation of SP-A#, and thus promotes aggregation of vesicles and the exchange. The selectivity of the exchange, and reversibility of the calcium-induced aggregation by the addition of EGTA, shows that the vesicle−vesicle contact formation is calcium dependent and reversible, and does not lead to a stable (hemi)fused state.

These results and the model are compatible with a role for SP-A in lipid 'trafficking and sorting' between the various alveolar compartments and for the recycling of the spent material. In this hypothesis, SP-A serves to deliver fresh DPPC and other lipid species from the hypophase to the monolayer and its return, steps necessary for the biophysical role of DPPC in the expansion−contraction cycle of the alveolar monolayer. SP-A could also mediate the exchange of lipid species between the alveolar hypophase and the epithelial cell membrane, thereby facilitating the surfactant recycling through membrane retrieval.

MATERIALS AND METHODS

Reagents. Pyrene-labeled phospholipids (PyPX = PyPC, PyPG, PyPE, PySM), ANTS, DPX, and R18 were from Molecular Probes. DPPC, POPC, POPG, DMPG, DNS-PE (egg), NBD-PE (dioleoyl-), and Rh-PE (dioleoyl-) labeled at the amino group of phosphatidylethanolamine were from Avanti. Dithionite (sodium hydrosulfite) was from Mallinckrodt Chemical Works (St. Louis). DTGPE-DNS was synthesized as described (*28*).

Most protocols and appropriate controls used in this study have been established before for monitoring phospholipid exchange (*18*−*27*). Only salient details are described below, and specific conditions are given in the figure captions. All manipulations were carried out in glass containers. Unless noted otherwise, all measurements were made in 100 mM NaCl, 0.05 mM EGTA, and 10 mM Tris at pH 7.4 with other additives as required. Fluorescence measurements were performed in a stirred quartz cuvette at 25 °C on an AB-2 spectrofluorimeter (SLM-Aminco). All spectral manipulations were carried out with the software provided with the instrument. Typically, the slit-widths were kept at 4 nm each, and the sensitivity (PMT voltage) was set for the buffer blank to 1% for the Raman peak corresponding to the same excitation wavelength. The excitation/emission wavelengths for the various probes are 346/396 nm for pyrene, 346/535 nm for dansyl, 556/577 nm for rhodamine, 450/535 nm for NBD, and 285/335 nm for tryptophan.

Isolation of SP-A. SP-A was isolated from human lung surfactant with the use of 1-butanol and *n*-octyl α-D-glucopyranoside extraction and dialysis according to the method of Hagwood et al. (*29*), and the purity was confirmed by the appropriate bands observed by SDS−PAGE electrophoresis (*30*). SP-A concentration was quantified by the Coomassie blue assay (Bio-Rad, Hercules, CA) with bovine γ-globulin as standard. Protein concentrations are expressed on the basis of the aggregate molecular mass, 660 kDa. The purified SP-A preparation in 10 mM Tris at pH 7.4 was stored frozen in small aliquots at −20 °C in sterile microtubes (from Starstedt Inc.). After thawing, solutions kept at 4 °C tended to show an increase in turbidity after 4 h, and quantitatively different behavior in the various assays. Conditions permitting, for the best results we used the SP-A samples within 4 h after thawing. Typically, the mixing order to the buffer was vesicles added first, followed by SP-A, and calcium added last. If probe vesicles were present, the donor and acceptor vesicles were allowed to equilibrate for about 60 s before the addition of other components. Independent controls showed that none of the probe lipids exchanged significantly in the absence of proteins.

Preparation of Sonicated Vesicles. Fluorescent probes (such as NBD-PE, Rh-PE, DTGPE-DNS, PyPX) were included during the formation of the probe vesicles at the indicated mole percent by replacing comparably charged anionic or zwitterionic species. In all cases, covesicles were prepared from the vacuum-dried film of the indicated lipids premixed in chloroform and methanol (3:2). The film was hydrated and then sonicated in a bath-type sonicator (Lab Supplies, Hicksville, NY; Model G112SPIT) above the gel−fluid transition temperature until a clear dispersion was obtained (typically 5 min). Vesicles were annealed for 30 min before use.

Unless indicated otherwise, covesicles were prepared with a mixture of DPPC, POPG, and cholesterol with the mole percent in the consensus range for the composition of the human lung surfactant (*31*). The following vesicles are referred in the text and figure captions: vesicle-1,75% DPPC, 15% POPG, and 10% cholesterol; DNSPE-vesicle, 12% DNS-PE (egg), 63% DPPC, 15% POPG, and 10% cholesterol; DTDNS-vesicle, 12% DTGPE-DNS, 63% DPPC, 15% POPG, and 10% cholesterol; NBD-vesicle, 0.6 or 2% NBD-PE, 73 or 74.4% DPPC, 15% POPG, and 10% cholesterol; PyPC-vesicle, 30% PyPC, 55% DPPC, 15% POPG; PyPE-vesicle 30% PyPE, 55% DPPC, 15% POPG; PyPG-vesicle, 30% PyPG, 60% DPPC, 10% cholesterol; PySM-vesicle, 30% PySM, 55% DPPC, 15% POPG; Rh-vesicle, 0.6 or 2%

RhPE, 73 or 74.4% DPPC, 15% POPG, and 10% cholesterol; R18-vesicles, 12% R18, 67% DPPC, 12% POPG, 9% cholesterol.

Light Scattering. The change in turbidity of vesicle-1 was measured as the change in the 90° scattered intensity at 400 nm with 1 nm slit-widths on a SLM-Aminco AB-2 spectrofluorimeter. Typically, an aliquot of sonicated vesicles was added to the cuvette containing buffer, and then SP-A was added from a stock solution, followed by $CaCl_2$. The change in scattering was monitored continuously over 20 min with 2 s resolution. The effect of $CaCl_2$ alone on the turbidity of the vesicles was negligible. Comparable conditions, at higher instrumental sensitivity, were used to monitor the calcium-induced turbidity change of SP-A in the aqueous phase.

Fluorescence Assays for Lipid Mixing. Unless indicated otherwise, all measurements were made with vesicle-1, and these vesicles were also used as acceptor vesicles for the exchange studies with the probe vesicles of the compositions described above. Control experiments showed that the spontaneous exchange of phospholipid and cholesterol with probes is negligibly slow in the absence of SP-A and calcium, and the exchange is triggered by calcium at concentrations that depend on the presence of NaCl.

(i) Monitored as Change in Monomer Emission of PyPX by Surface Dilution. The exchange of lipid between vesicles, typically on the addition of SP-A followed by calcium, was assessed by monitoring the dilution of pyrene-vesicles mixed with an 125-fold excess of vesicle-1 as acceptor. Emission was monitored at 395 nm (with excitation at 346 nm), corresponding to the monomer emission.

(ii) Monitored as Release of Self-Quenching of R18 or Dansylated Phospholipid. Lipid mixing induced by SP-A was monitored with 30% probe containing R18-, DTDNS-, or DNSPE-vesicles mixed with vesicle-1 in a 1:125 mole ratio. The fluorescence increase was due to probe dilution upon exchange induced by SP-A without or with $CaCl_2$ in the medium.

(iii) Resonance Energy Transfer (RET) from Dansyl Donor to Rhodamine Acceptor. The emission from 12% probe containing DNSPE- or DNSPE-vesicles was used for energy transfer to Rh-vesicles. The energy transfer induced by SP-A under suitable conditions is shown by an increase in the rhodamine signal at 592 nm, or a much larger decrease in the dansyl signal at 535 nm (excitation 346 nm).

(iv) RET from NBD-PE Donor to Rh-PE Acceptor. SP-A-mediated mixing of probes between NBD-vesicles and Rh-vesicles (1: 1 ratio) with 0.6% probes was monitored as a decrease in the donor emission at 535 nm or as an increase in the acceptor emission at 592 nm with excitation at 460 nm. The maximum signal after total mixing was measured with covesicles containing 0.3 mol % of each of the probes at the same bulk lipid concentration. The signal at 592 nm usually has a contribution from NBD, and thus the observed change is somewhat affected by the decrease in the NBD signal. No attempt was made to resolve the individual contributions.

Vesicle−vesicle apposition without exchange of phospholipid was monitored by the RET protocol by taking advantage of the fact that NBD-PE and Rh-PE do not exchange in the probe dilution protocol described above in (iv). The RET signal by apposition of vesicles without lipid mixing is much lower than the signal that accompanies lipid mixing; therefore, equal concentrations of the 2% NBD-vesicles and 2% Rh-vesicles were used to monitor the apposition induced by SP-A with a decrease in the NBD emission as the RET signal.

Dithionite Assay To Determine the Accessibility of Phospholipid in Covesicles. Reaction of small sonicated vesicles containing NBD-PE with dithionite selectively eliminates the fluorescence signal derived from NBD present in the outer leaflet by a reduction reaction (*19*, *20*). An aliquot of 0.6% NBD-vesicles was added to 1.5 mL of 10 mM Tris, 0.05 mM EGTA, 0.1 M NaCl buffer at pH 7.4 saturated with nitrogen, with constant stirring (lipid concentration 11 μM). When a stable base line was achieved (usually less than 60 s after the addition), the reaction was started by adding dithionite from a stock solution to a final concentration of 10 mM. The time-dependent decrease in the fluorescence at 535 nm was recorded for 800 s (resolution 2 s). The Excitation wavelength was set at 460 nm with both slit widths at 4 nm. Stock solutions of freshly prepared 1.44 M dithionite in 0.5 M Na_2CO_3 (pH 11) buffer saturated with nitrogen gas were stored at 0 °C and used within 1 h.

Binding of SP-A to Vesicles. Two different protocols were used to monitor the binding. For RET measurements, tryptophan donors of SP-A bound to vesicles containing 2% NBD- or DNS-vesicles give maximum emission in the 490−550 nm range with excitation at 285 nm. Also, binding of SP-A, with an intrinsic tryptophan florescence emission maximum at 337 nm, to vesicles is accompanied by a shift to 332−333 nm. Typically these measurements were carried out with 100−600 μM phospholipid as vesicles in 1.5 mL of buffer with 40−80 μg of SP-A and other additives as indicated. Specific conditions are given in the figure legends. Casals et al. (*14*) report somewhat different intrinsic fluorescence emission properties of SP-A with two emission peaks at 326 and 337 nm, suggesting the presence of a mixture of SP-A populations. This may also be responsible for a difference in the initial time course of the aggregation kinetics.

Although details are not conclusively established, it appears that the starting state of SP-A in the stock solutions changes significantly with the buffer conditions and the presence of trace amounts of calcium. The turbidity changes in SP-A stock solutions kept at 4 °C are best monitored as the RET signal from Trp of SP-A to NBD-PE in vesicles in the absence of NaCl and $CaCl_2$. We believe that such uncontrolled variables, associated with the aggregation of SP-A in the aqueous phase, are responsible for anomalous results, and could account for minor quantitative differences in our intrinsic fluorescence results compared to those reported by Casals et al. (*14*).

RESULTS

Phospholipid Exchange by SP-A Occurs Only in the Presence of $CaCl_2$. Fluorescence changes from dequenching of rhodamine, dansyl, or pyrene lipids, and also the RET signal from mixing of NBD- or dansyl-probes with Rh-probes, were used to monitor the time course of exchange of the probes between vesicles. In addition to the effect of reactant concentrations (Scheme 1), calcium is required for probe exchange, and the effect is enhanced in the presence

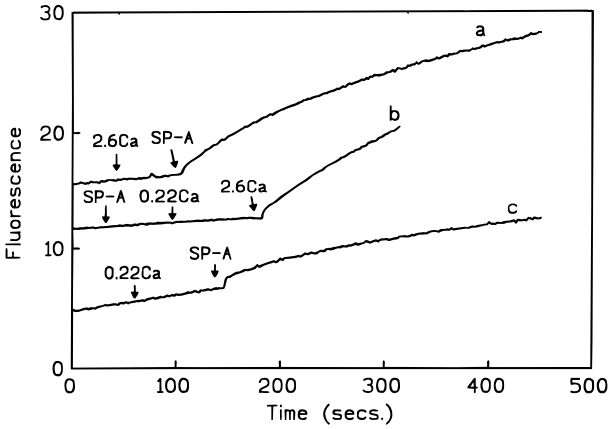

FIGURE 1: Effect of SP-A (40 μg or 40 nM) and calcium (as indicated) on the time course of the fluorescence increase due to the surface dilution of R18 on intervesicle exchange of the probe. The aqueous phase consists of 1.5 mL of 10 mM Tris and 0.05 mM EGTA at pH 7.4 and 24 °C with (curves a and c) or without (curve b) 0.1 M NaCl. The sequence of addition was acceptor vesicle-1 and donor 12% R18-vesicles in a 125:1 ratio followed by (a) 2.6 mM $CaCl_2$ and then SP-A; (b) SP-A followed by 0.22 mM and then 2.6 mM $CaCl_2$; (c) 0.22 mM $CaCl_2$ followed by SP-A. The total lipid concentration was 215 μM. Note that the slow background level of the fluorescence change due to a slow exchange of R18, which contains a single octadecyl chain, with acceptor vesicles is noticeable in this assay. Note that curves are displaced vertically for clarity.

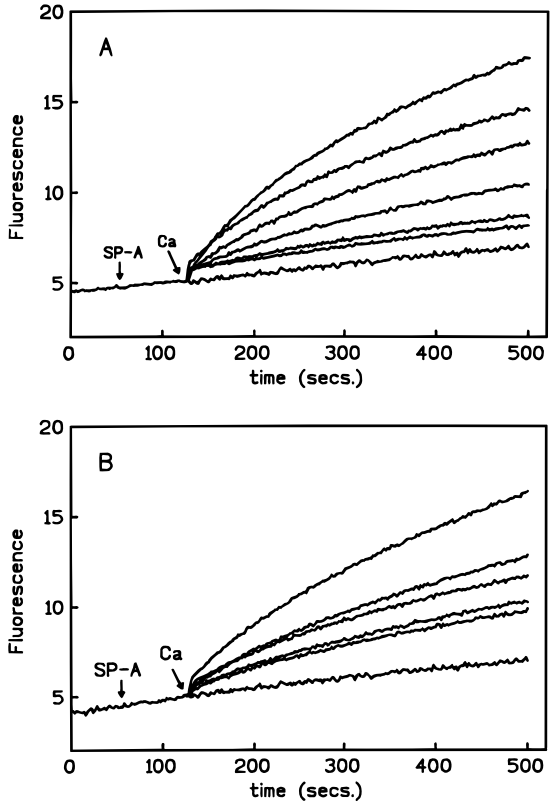

FIGURE 2: Effect of (A) calcium or (B) SP-A concentration on the time course of R18 exchange in 1.5 mL of 10 mM Tris and 0.1 M NaCl and other conditions as in Figure 1. (A) Effect of (from top) 2.67, 2.0, 1.33, 0.667, 0.266, 0.133, and 0 mM $CaCl_2$ at 40 nM (or 40 μg) SP-A. (B) Effect of (from top) 80, 60, 50, 30, 20, and 0 μg of SP-A at 0.32 mM $CaCl_2$. Other conditions as in Figure 1.

of 0.1 M NaCl. As shown in Figure 1, at 0.22 mM Ca the fluorescence increase due to the dilution of R18 is induced by SP-A only in the presence of NaCl (curves b versus c). At 2.6 mM Ca, the dequenching rate is higher and seen in the presence (curve a) or absence (curve b) of NaCl. The order of rapid addition (<1 min) of calcium and SP-A does not appear to be qualitatively critical; however, the shape of the reaction progress was found to change significantly with longer periods of preincubation. The lipid mixing is observed virtually instantaneously after the addition of the last necessary component, typically calcium. The fluorescence increase induced by SP-A does not reach a plateau, although the mixing stops immediately on the addition of EGTA (see below). Even after 30 min of mixing the signal is <15% of the maximum signal seen after complete dilution of the probe in the presence of deoxycholate. Higher rates of mixing were seen at lower pH (4.5), where addition of calcium did not have a significant effect (results not shown nor investigated in detail).

The dependence of R18 dilution as a function of [$CaCl_2$] at 40 nM SP-A is shown in Figure 2A. At low concentrations, the effect on the progress curve appears modest because the buffer contains 0.05 mM EGTA. The initial slope saturates at 2 mM calcium, presumably because the calcium-dependent rate of exchange through the contact saturates. The extent of mixing at longer times does not apparently saturate even at 2.6 mM. It suggests that a secondary process, such as the exchange of vesicles in contact through SP-A, may not be calcium dependent. As shown in Figure 2B, the apparent rate and extent of exchange at constant [Ca] increase with [SP-A]. At SP-A/vesicle ratios $\ll 1$, this is expected as excess vesicles form new SP-A contacts for the dilution of the probe.

Specificity of Exchange of Labeled Phospholipid. The exchange specificity for the phospholipid probes is shown

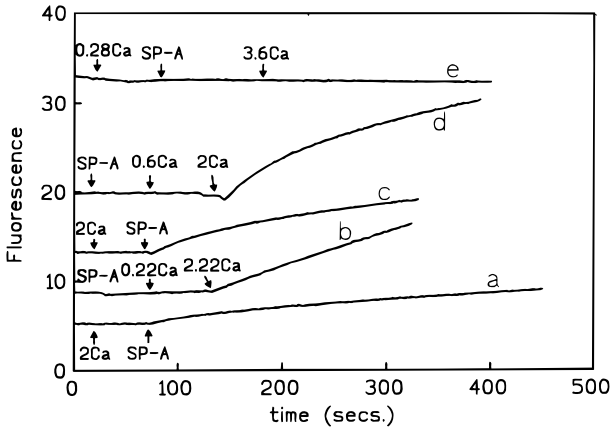

FIGURE 3: Effect of SP-A (80 μg for curves a−d, and 40 μg for curve e) and calcium with 0.1 M NaCl on the time course for the exchange of probe lipids with vesicle-1 as acceptor. From bottom: (a) 3 mM calcium followed by SP-A is added to a mixture of PySM-vesicles and vesicle-1 (1:125 ratio); (b) SP-A followed by 0.22 and 2.2 mM calcium to mixture of PyPG-vesicles and vesicle-1; (c) 2 mM calcium followed by SP-A to PyPC-vesicles and vesicle-1; (d) SP-A followed by 0.6 and 2 mM calcium added to PyPE-vesicles and vesicle 1 (2:215 μM); (e) 0.28 mM calcium followed by SP-A and 3.6 mM calcium added to 0.6% NBD-vesicles and 0.6% Rh-vesicle (66 μM each). Excitation 346 nm and emission 396 nm for pyrene lipids, and 460/535 nm for NBD.

by several assays. The SP-A-mediated exchange of pyrene-labeled phospholipid, PyPX, was not seen at 0.22 mM Ca in 0.1 M NaCl, yet a significant exchange of PySM, PyPG, PyPC, and PyPE is observed at 2.6 mM $CaCl_2$ (curves a through d in Figure 3). The various orders of mixing in

Table 1: Apparent Initial Rate of SP-A-Mediated Exchange of Phospholipid Probes with Vesicle-1[a]

donor	$10^4 \times \delta F/F_{max}$	rate (s^{-1})	donor	$10^4 \times \delta F/F_{max}$	rate (s^{-1})
PyPC-vesicle	2.5	0.75	R18-vesicle	0.94	0.3
PyPG-vesicle	2.1	0.63	DNSPE-vesicle	18	6
PyPE-vesicle	5.0	1.5	NBD-vesicle	0.1	0.03
PySM-vesicle	1.1	0.33	DNS-PE/POPC[b]	2	0.5

[a] Probe vesicles contain 30 mol % probe with 55% DPPC and 15% POPG, and vesicles-1 are used as acceptor vesicles. Dequenching was initiated with 3.0 mM $CaCl_2$ added to a mixture of 2.4 nmol of lipid as probe vesicle, 320 nmol of lipid as acceptor vesicle-1, and 80 μg (120 pmol) of SP-A in 0.1 M NaCl and 10 mM Tris at pH 8.0. The standard deviation in $\delta F/F_{max}$ is <10% ($n = 3$). Other conditions as in Figure 3. F_{max} was determined after the addition of 3 mM deoxycholate at the end of the exchange reaction. [b]Both the acceptor and donor vesicles contain only POPC.

this assay also provide controls which rule out a direct effect of calcium on the vesicles to promote lipid mixing, e.g., by fusion. The apparent initial rate of mixing is different for the various probes, which also rules out the possibility of calcium-induced (hemi)fusion. The cholesterol-containing vesicles-1 were used as acceptor in all of the studies in Figures 1−3. The donor vesicles also contain cholesterol, with the exception of PyPC, PyPE, and PySM vesicles. A qualitatively comparable exchange profile was seen with cholesterol-free and cholesterol-containing donor−acceptor vesicles containing DPPC and POPG (results not shown). These results rule out the possibility that the PyPX exchange somehow depends only on the presence of cholesterol. Also, spontaneous exchange of cholesterol from donor vesicle-1 to cholesterol-free acceptor vesicles was deemed negligible, because there is no other exchangeable species present in the acceptor vesicles to compensate for the transfer of cholesterol.

Results in Figure 3 (curve e), with 0.6% NBD-PE (acceptor) and 0.6% Rh-PE (donor) vesicles, show that neither probe mixes with the other in the presence of SP-A and 3.6 mM Ca. On the other hand, selective exchange of dansyl-PE is mediated by SP-A with a characteristic calcium concentration dependence. As shown in Figure 4A, the increase in the signal due to dequenching of DTGPE-DNS is seen only at 3.3 mM Ca (bottom curve), whereas the egg DNS-PE exchanges even at 0.22 mM Ca (top curve). Also as summarized in Table 1, both the extent and rate of dequenching of DNS-PE in POPC vesicles are significantly lower. Comparable experiments with NBD-PE showed no dequenching signal with vesicle-1 induced by SP-A at 0.22 or 2.6 mM $CaCl_2$ (e.g., see curve e in Figure 3). These results suggest SP-A-mediated exchange of DNS-PE, but not of NBD-PE or Rh-PE, indicating a headgroup specificity for the exchange.

The fluorescence emission from DNS-PE in the 480−550 nm region has a significant overlap with the excitation of rhodamine at 530−570 nm. The emission spectrum of a mixture of DNSPE-vesicles with 2% Rh-vesicles shows a larger decrease in the donor signal in the 540 nm region and a modest increase in the acceptor signal in the 592 nm region. The profiles in Figure 4B show that SP-A-mediated phospholipid exchange, monitored as a decrease in the RET donor (lower pair of curves) or as an increase in the RET acceptor (upper pair of curves), is seen in the presence of 0.22 mM $CaCl_2$, and the rate is noticeably more rapid at 3.3 mM.

The exchange selectivities for the probes used in Figures 2−4 were compared under identical conditions (Table 1), except for the results in the last row where only POPC is present in the probe and acceptor vesicles. In all cases, the

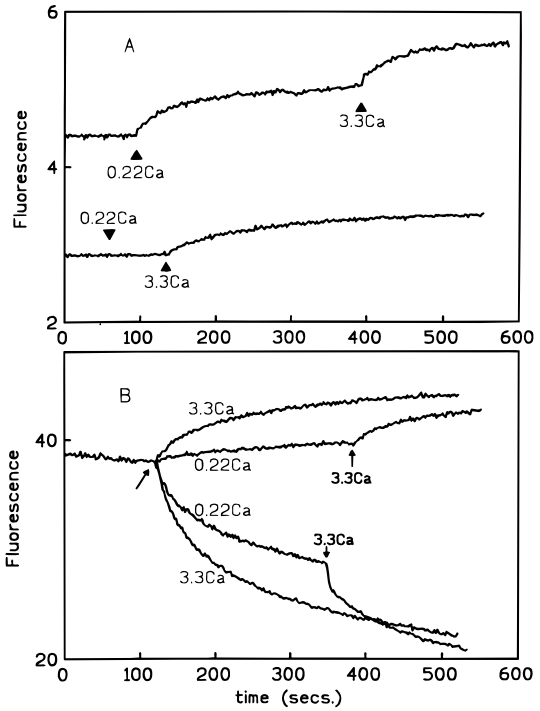

FIGURE 4: (A) Effect of SP-A (80 μg) and calcium on the time course of dequenching from surface dilution of the dansyl lipid after exchange with vesicle-1. (Top) SP-A followed by 0.22 and 3.3 mM calcium added to the mixture of 30% DNSPE-vesicle and vesicle-1 (1:133 ratio with 215 μM total lipid); (bottom) SP-A followed by 0.22 and/or 3.3 mM calcium added to the mixture of 30% DTGPE-DNS-vesicle and vesicle-1 (1.6 μM to 210 μM). Excitation 346 nm and emission 530 nm. (B) Effect of SP-A and calcium on the time course of mixing of Rh- and DNS-PE monitored as the decrease in the dansyl donor signal at 535 nm or as the increase in the rhodamine acceptor signal at 592 nm due to resonance energy transfer. SP-A (8 μg), added to a mixture of 12% DNSPE-vesicle and 2% Rh-vesicle (6.6 μM each), followed by 0.22 and 3.3 mM calcium (for the inner profiles), or only 3.3 mM calcium for the outer profile.

dequenching is due to the exchange of the probe from the 30 mol % probe vesicles to the acceptor with 80 μg of SPA at 3 mM $CaCl_2$. The initial rate of the fluorescence change as a function of the maximum signal obtained by the addition of deoxycholate, $\delta F/F_{max}$, for the various probes differs significantly. Since only the contacts of the probe-containing vesicles with the probe-free vesicles give the dequenching signal, the absolute rate of exchange can be calculated with certain assumptions. This assay mixture contains 2500 pmol of vesicles per 120 pmol of SP-A. A Poissonian excess of vesicles implies that most vesicles in contact contain at most the minimum number of SP-A molecules per contact, which we assume to be one SP-A per contact between two vesicles. For a vesicle containing 10 000 phospholipids, 3000 probe

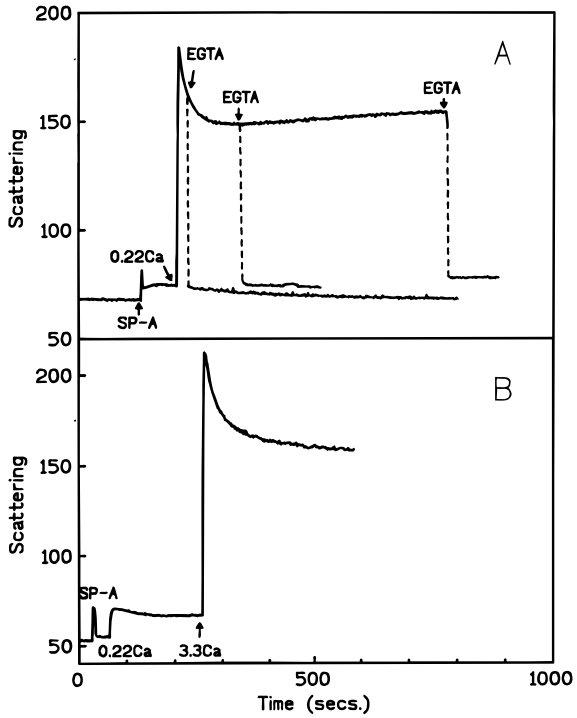

FIGURE 5: (A) Changes in the intensity of 90° scattered light at 400 nm of vesicle-1 (215 μM) in 0.1 M NaCl by SP-A induced by 0.22 mM free $CaCl_2$ added at 100 s in the presence of 0.04 μM SP-A added at 65 s. In separate runs, 0.3 mM EGTA was added at 20, 140, or 770 s after the addition of calcium. (B) Effect of SP-A and calcium on the scattered light intensity in the same buffer but without NaCl. Other conditions as in Figure 1.

molecules from the probe vesicle are diluted into vesicle-1. Thus, the initial dequenching rate, $\delta F/F_{max}$, of 10^{-4} per second corresponds to a rate of 0.3 per second. This is only a lower limit estimate for the apparent initial rate of exchange made with the assumption that other phospholipid molecules do not inhibit by competing with the probe for the exchange.

The key conclusion of the probe transfer studies in Figures 1−4 is that SP-A and calcium induce the probe exchange. Specificity for the exchange is shown by the limit estimates for the apparent initial rates summarized in Table 1. Both the extent and the initial rate of the exchange depend on the calcium and the SP-A concentration in the presence of NaCl. If a certain cluster-size is preferred, as seen with polymyxin B (*24*), such a model is not readily amenable to quantitative analysis in terms of the primary rate and equilibrium parameters for contact formation (Scheme 1). However, to establish the experimental boundary conditions for the characterization of the contacts, rationalized in terms of Scheme 1, we qualitatively characterize the variables that control the observed kinetic behavior.

Vesicles Aggregate in the Presence of SP-A and Calcium. The effect of SP-A on the aggregation of vesicles has been extensively characterized (*2*, *12*). We present key results relevant for the interpretation of the probe exchange results, i.e., the aggregation step that precedes the exchange in the last step (Scheme 1). Apposition of donor−acceptor vesicles is critical for phospholipid exchange, and the resulting increase in the apparent size is accompanied by a change in the 90° light scattering. Results in Figure 5 show a very rapid and large increase in the scattering of vesicle-1 induced by SP-A in the presence of 0.22 mM calcium plus NaCl. The steady-state change in the scattering of POPC or DOPC vesicles is considerably smaller (results not shown) as the initial increase relaxes to the starting intensity with a half-time of about 30 s. This behavior accounts for the rapid initial rate of probe exchange, followed by a decrease in the apparent extent of the exchange. Although we have not investigated this phenomenon in detail, results at hand suggest that the nature of the phospholipid determines the partitioning of the aggregated vesicles into a exchange-competent species, or its reversal to a calcium-dependent aggregated form of SP-A (see below).

The magnitude of the scattering change at constant SP-A and calcium concentrations is considerably smaller in the absence of NaCl. For example, the intensity at 3.3 mM calcium in the absence of NaCl (Figure 5B) is comparable to that induced with 0.22 mM calcium in the presence of 0.1 M NaCl (Figure 5A), as also seen for the exchange. The magnitude of the scattering change increases with the concentration of SP-A and calcium (summarized later in Figure 10). The calcium-induced change is rapidly reverted on the addition of EGTA: at short time intervals after the addition of calcium, the signal reaches the same level as before the addition of calcium; after long periods of incubation with calcium, the EGTA-dependent reversal does not reach the initial level. The overall scattering change consists of three time-dependent processes with half-times of about 3 (rise), 30 (short drop), and >300 s based on the residual scattering after the addition of EGTA at different time points in the aggregation profile. Note that the initial rise phase of the scattering change is much more rapid than in the probe exchange profile. The two slower processes have an apparent relationship to the probe exchange and the exchange of vesicles in contact; however, we do not have any direct evidence. These results show that although aggregation and probe exchange occur under comparable conditions, the exchange is considerably slower, and that the exchange is accompanied by only a modest change in the scattering after the initial burst.

Apposition of Vesicles Is Induced by SP-A. Apposition of 2% NBDPE-vesicle donor to 2% Rh-vesicle acceptor for RET induced by SP-A and calcium was established by the protocol used to show the vesicle−vesicle apposition induced by the myelin basic protein (*27*) and mellitin (*26*). Addition of calcium causes a rapid decrease in the NBD-PE emission and a parallel increase in the Rh-PE emission only in the presence of SP-A and NaCl; the RET signal from apposed vesicles reverts on the addition of excess unlabeled vesicles or EGTA (results not shown). Although we have not investigated in detail, the steady-state time course suggests that among other factors the exchange of vesicles in contact occurs on the time scale of several minutes, and that the apparent exchange rates depend on the composition of the donor and acceptor vesicles. Both lipid mixing and fusion are discounted by the results described above, showing that neither of these probes exchange under these conditions.

Mixing of Lipids of Apposed Vesicles Occurs Without Flip-Flop or Disruption of the Vesicles. SP-A did not disrupt vesicles under the conditions used for the probe exchange studies. This is demonstrated by the fact that the addition of dithionite to 0.6% NBD-PE vesicles, with or without SP-A or calcium, results in a partial decrease in the fluorescence from NBD (Figure 6). The reaction starts immediately after

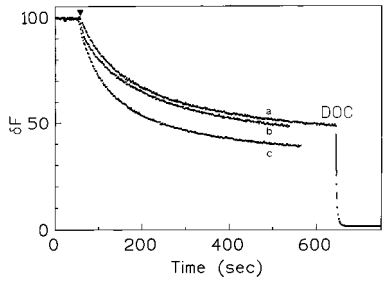

FIGURE 6: Time course for the loss of fluorescence of NBD-vesicles (11 μM total lipid) by 10 mM dithionite added at 60 s in 0.22 mM calcium in the (curve a) absence or (curve b) presence of 2 μg of SP-A added at 10 s; (curve c) the probe vesicles were incubated with 8 μg of SP-A and 2.6 mM calcium for 30 min before initiating the reaction with dithionite. Addition of deoxycholate (DOC) in curve a at 650 s caused leakage of vesicles.

the addition of dithionite, and the time course has two components (*26*, *27*): a fast phase, which is complete in about 100 s, is due to the reduction of the exposed NBD-PE in the outer monolayer of the vesicles. A parallel but considerably slower decrease in the NBD fluorescence is possibly due to the permeation of dithionite and reduction of NBD-PE in the inner monolayer. Results in Figure 6 show that the fraction of NBD-PE quenched by dithionite does not change with 0.2 mol % SP-A and 0.2 mM calcium (curves a and b). Also a modest increase in the dithionite-quenched signal in the initial rapid phase is seen after the incubation of vesicles with 0.55 mol % SP-A in the presence of 2.6 mM calcium (curve c); however, the extent of quenching does not depend on the time of incubation. These results rule out SP-A-mediated vesicle leakage or solubilization, and suggest that even under the extreme conditions used in this study only a very small change in dithionite-accessible NBD-PE is promoted by SP-A.

Leakage of water-soluble self-quenched probes trapped in vesicles was also monitored on the addition of SP-A. These protocols (*26*, *27*) provided independent evidence that 80 μg of SP-A, added to 12.5 mM ANTS and 45 mM DPX cotrapped in 360 nmol of phospholipid as vesicle-1 in 1.5 mL of buffer, does not cause any noticeable (<1%) release even after 15 min incubation in the presence or absence of calcium.

The Tryptophan Environment of Bound SP-A Depends on the Lipid Composition. SP-A monomers contain 2 tryptophan residues: Trp-2 and Trp-248 in the 263 residue chain. Binding of SP-A to vesicles is readily monitored as the resonance energy transfer signal from Trp donor to a DNS or NBD acceptor localized in the vesicle interface. As shown by the difference spectra in Figure 7A, obtained in the absence of $CaCl_2$, the RET signal from DTGPE-DNS on saturated DPPC and DTPM vesicles is considerably larger than the signal from the dansyl probe on unsaturated POPC or DOPC vesicles where the signal is barely above the background level. Similarly, in the presence of 0.22 mM calcium, the intensity of the RET signal is significantly larger at all four interfaces (Figure 7B). A comparable calcium-dependent increase is also seen if calcium is added to the mixture of SP-A and vesicles. The change in the intrinsic fluorescence of Trp on the binding of SP-A to interfaces is shown in Figure 8. A decrease in the Trp emission is seen in all cases, but the change is larger with anionic and saturated phospholipid. Note that the direction of the change

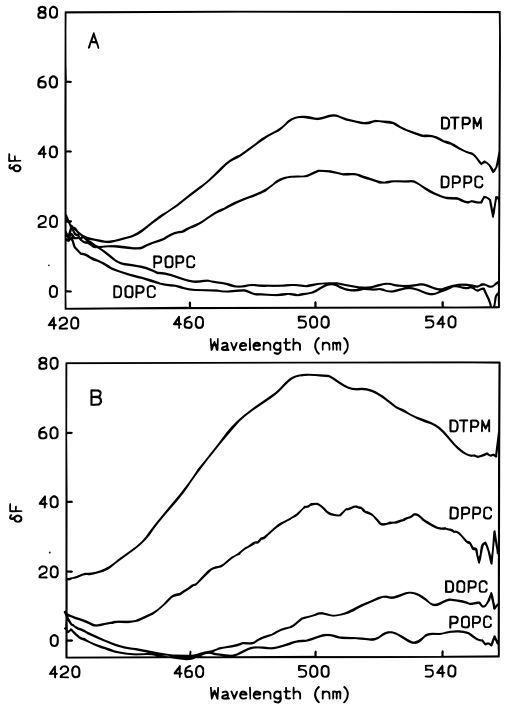

FIGURE 7: (A) RET difference spectra on the binding of 0.04 mg/1.5 mL SP-A added to 0.1 mM DTPM, DPPC, POPC, or DOPC vesicles containing 2% DTGPE-DNS in buffer without calcium. (B) Changes in the RET difference spectra [as in (A)] in the presence of 0.22 mM calcium. Excitation 285 nm.

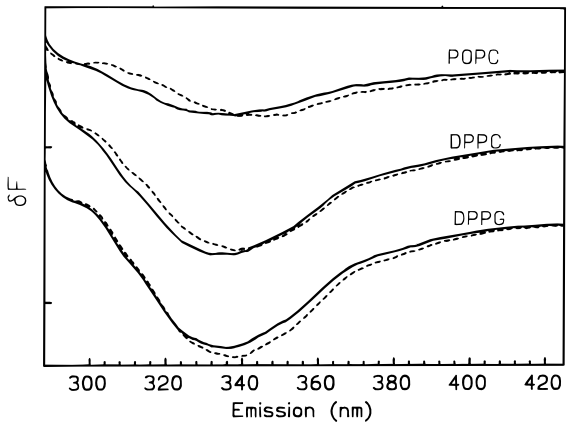

FIGURE 8: Effect of 0 (solid lines) or 0.22 mM free calcium (dashed lines) on the tryptophan fluorescence emission difference spectra of 0.1 mg of SP-A resulting from the addition 0.425 mM (top) POPC, (middle) DPPC, and (bottom) DPPG as vesicles. The spectra are shifted on the ordinate for clarity; however, the intensity at 420 nm represents 0% change in each case. The markings on the left ordinate represent a 50% change in the fluorescence.

in the Trp signal is opposite to the change in the RET signal. The magnitude of the change observed in both assays with the various essentially single phospholipid vesicles is in the same rank order; i.e., irrespective of the charge, the saturated lipids exhibit a larger magnitude of the change, and in all cases, the spectral signatures are modulated by calcium. These results show that the binding of SP-A does not require calcium, although calcium does change the difference spectrum. In conjunction with a quantitative specificity for the phospholipid composition, these results suggest that SP-A binding is a necessary but not a sufficient condition for probe exchange.

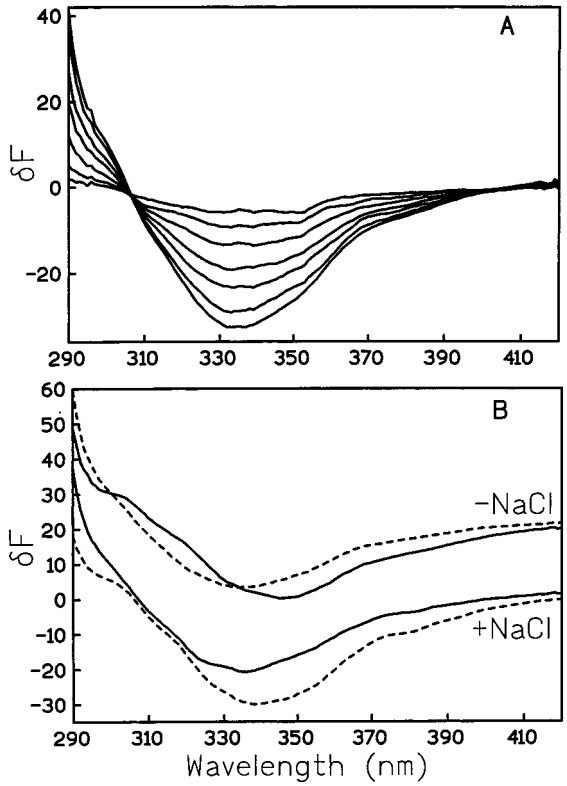

FIGURE 9: (A) Effect of total lipid concentration (from the bottom; 0.8, 0.66, 0.46, 0.33, 0.186, 0.08, and 0.026 mM) added successively as vesicle-1 on the Trp difference spectra. (B) Effect of (upper set, shifted up for clarity) 0 or (lower set) 0.1 M NaCl in 10 mM Tris at pH 7.4 on the tryptophan emission difference spectra induced in 0.1 mg of SP-A in (solid) 0 or (dashed) 0.22 mM free $CaCl_2$ on the addition of 0.425 mM lipid as vesicle-1. Other conditions are as in Figure 7.

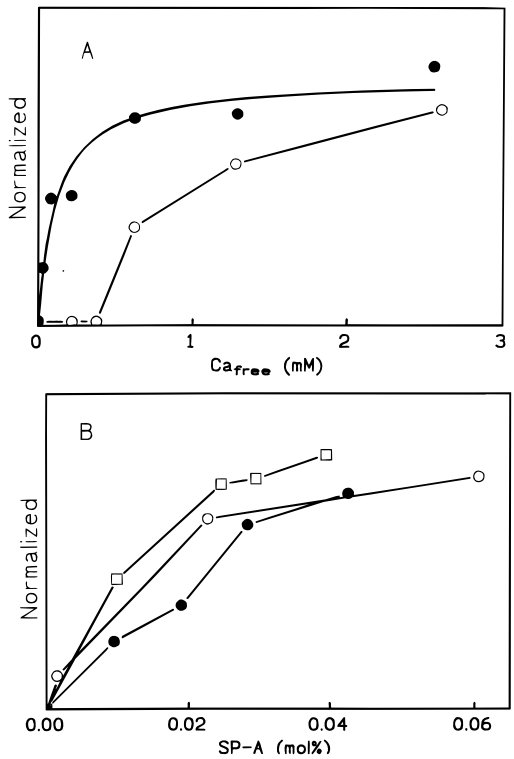

FIGURE 10: (A) Calcium concentration dependence of the (solid circles) extent of aggregation and (open circles) the initial rate of exchange of PyPC between PyPC-vesicles and vesicle-1. Other conditions as in Figures 3 and 5. (B) SP-A concentration dependence of the extent of scattering (solid circles) and the initial rate of exchange of R18 (squares) or DNSPE-egg (open circles) with vesicle-1 at 0.22 mM $CaCl_2$. All values are normalized to the same maximum. Other conditions as in Figures 2A, 4B, and 5.

Complementary information on the binding of SP-A to vesicle-1, with the composition in the consensus range for the lung surfactant, is provided by the Trp emission spectra shown in Figure 9. Results in Figure 9A show that at near-optimal levels of calcium and NaCl for probe exchange, only the intensity, but not the shape, of the difference spectra changes with the amount of phospholipid added as vesicle-1. This is expected for a simple equilibrium binding of SP-A from the aqueous phase to the interface, and a well-defined isosbestic point indicates that the underlying change involves only two major spectroscopic species in equilibrium. The change in the intensity at 333 nm with vesicle concentration could not be satisfactorily fitted to a single hyperbola, which implies the existence of other competing equilibria.

The shape of the spectral change in the Trp emission on the binding of SP-A to vesicle-1 is modestly affected by calcium and NaCl (Figure 9B). The results are consistent with the kinetic results which show that the effect of SP-A at low calcium is significantly modulated by the presence of NaCl. It is difficult to interpret these changes because NaCl and Ca have a significant effect on the Trp emission from SP-A in the aqueous phase (results not shown). Also, the bulk phospholipid concentration dependence of the decrease in the intensity is comparable in the presence or absence of NaCl; however, quantitative results are somewhat uncertain because the change is slow and time dependent in the absence of NaCl. Although we have studied only the short-time effects, we suspect that, both in the aqueous phase and in the interface, SP-A is distributed in several species which under certain conditions equilibrate on the longer time scale.

In short, the SP-A binding results in Figures 7−9 show little specificity for the phospholipid composition of the interface; however, spectral signatures and the magnitudes of the changes suggest a range of bound SP-A conformers or aggregates. The fact that the Trp emission intensity decreases on the binding of SP-A to vesicles suggests that the changes in the Trp emission may be due to a significant change in the internal quenching environment of the two tryptophans, and that the magnitude of the decrease depends on the structure of the phospholipid. Thus, the increase in the resonance energy transfer intensity, despite a decrease in Trp emission on binding to vesicles, implies that the donor−acceptor distance for SP-A at the interface is sufficiently small, or the two spectral effects may be from the two different tryptophan residues.

Dependence of the Lipid Exchange on Calcium and SP-A Concentrations. We have not been able to quantify the effects of all the variables that control the SP-A-mediated exchange of phospholipid probes, and thus we are not in a position to analyze the results in terms of a unique kinetic model based on Scheme 1. Since most of the results were obtained under standard conditions, it is possible to evaluate effects of the two key variables. The effects of calcium and SP-A concentrations on some of the measured quantities (Figure 10) are revealing. The calcium concentration dependence of the extent of the light scattering change is

quite different than that for the exchange of PyPC (Figure 10A), which suggests that the aggregation and exchange steps are decoupled at least under certain conditions. Interestingly, R18 and DNS-PE exchange is seen at lower calcium concentrations, whereas NBD and Rh probes do not exchange even at 3 mM calcium (Figures 1−4). While these results clearly rule out lipid mixing due to (hemi)fusion, the calcium concentration dependence of the apparent exchange specificity may reside in, or be related to, the effect of calcium on the effective exchange rate as determined by the lifetimes of the aggregate and the contact. Such factors cannot be resolved yet.

Information about the SP-A/vesicle stoichiometry in the contact that mediates the exchange is intrinsic in results in Figure 10B. The extents of exchange of R18 and DNS-PE, as well as that of the scattering, saturate at about 0.025 mol % SP-A, i.e., at about 1 molecule of SP-A per 4000 phospholipid molecules. Since sonicated vesicles are expected to contain 4000−10 000 phospholipid molecules, these results imply that on an average 1 molecule of SP-A per vesicle forms a contact capable of mediating the phospholipid exchange. Since the scattering and the exchange of the two probes show the same SP-A/vesicle stoichiometry, these results also suggest that virtually all contacts are exchange-competent. Considering a Poisson distribution of SP-A over the vesicle population, these results suggest that either the disaggregated SP-A forms the exchange-competent contacts or, more likely, the vesicle aggregate is stable as clusters containing several contacts, each with one SP-A molecule.

Effect of Calcium on SP-A in the Aqueous Phase. The Origin of the calcium effect on vesicle aggregation and probe exchange can be traced to a direct effect of calcium on SP-A. The calcium-dependent shift in the SP-A to SP-A# equilibrium is accompanied by a change in its fluorescence spectrum, where the difference spectrum shows a 5% decrease in the peak intensity at 320 nm. As shown in Figure 11A, 1.2 mM calcium induces a biphasic change in the 90° scattering of SP-A in 0.1 M NaCl. The amplitude of the peak intensity and the final intensity shows a hyperbolic dependence on the free calcium concentration (Figure 11B) with an apparent dissociation constant of 0.3 mM, which is only slightly higher than the value of 0.2 mM (Figure 10A) for the scattering change associated with the aggregation of vesicles. Note that due to the sequential nature of these equilibria, there is an apparent synergistic effect on the calcium dependence monitored at different points along the equilibria in Scheme 1. These and other results (*6, 7*) suggest that the calcium induced change in SP-A is a prelude for interaction with a lipid interface followed by aggregation. In the absence of an interface, SP-A# self-aggregates. To what extent the lipid interface and other physiological variables determine the partitioning of SP-A# into a functional contact of self-aggregation remains to be established.

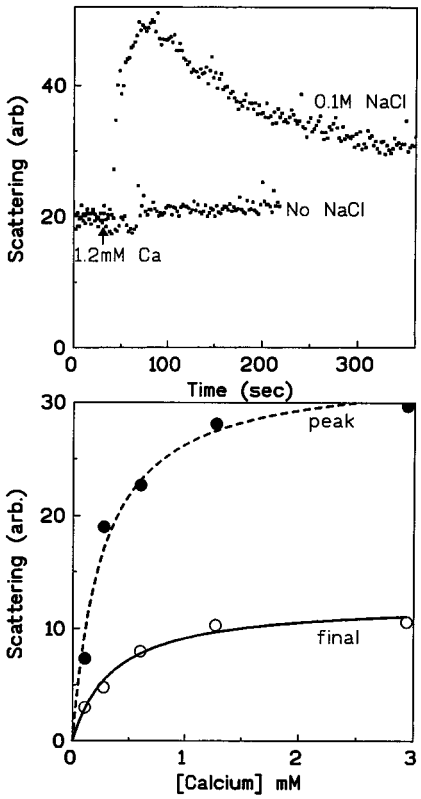

FIGURE 11: (A) Time course of the change in the 90° scattering at 400 nm induced by 1.26 mM free calcium added at 40 s to 20 μg of SP-A in 1.5 mL of Tris at pH 7.4, 0.1 M NaCl, and 0.05 mM EGTA without or with 0.1 M NaCl. Other conditions as in Figures 3 and 5. Aggregation of SP-A is also seen in the absence of NaCl at >2 mM Ca. (B) Peak and final scattering intensities of 20 μg of SP-A plotted as a function of free calcium. The apparent dissociation constant from the hyperbolic fit is 0.3 mM (SD 30%).

DISCUSSION

Many physiological functions involve contact between two membranes, such as vesicle formation, fusion, budding, targeting, endo- and exocytosis, fertilization, cell division, and vesicular transport of newly synthesized lipids and proteins to their final destinations within the cell (*32*−*34*). Selective transfer of phospholipids between the various compartments of a cell as well as in the extracellular space, sorting and trafficking as it is sometimes called, is an outstanding unresolved problem in cell biology that has generated considerable recent interest. Although many details remain obscure, it is believed that all the vesicular uptake processes utilize the same or very similar molecular machinery, and that specific proteins facilitate merger of lipid membranes, target selection, and regulation of fusion (*34*−*40*). According to an alternative mechanism, phospholipid exchange proteins promote selective exchange of phospholipid between membranes by binding and then ferrying a molecule of phospholipid through the aqueous phase (*41*, *42*). Obviously, certain yet unknown constraints must control the fluxes of components present in the donor and acceptor membranes, so that their compositional identity is not compromised. A fundamentally different process, specific contact-mediated exchange with SP-A and other proteins (*23*−*27*), offers an alternative.

Contact-Mediated Phospholipid Exchange. Direct and selective intervesicle exchange of phospholipid through protein-mediated contacts is a novel yet complex fundamental biophysical process whose significance is not widely appreciated. It is a useful paradigm for understanding the selectivity and control of phospholipid transfer during sorting and trafficking (*23*, *43*). Steps leading to the exchange have also been dissected for polymyxin B-mediated selective

exchange of monoanionic phospholipid (*23*−*25*), salt-triggered phospholipid exchange mediated by myelin basic protein (*27*), and mellitin-mediated exchange of zwitterionic phospholipid even though an anionic interface is required for the contact formation (*26*). The phospholipid transfer function of these peptides and proteins is critical for their putative biological function, as suggested by the specificity of the donor and acceptor interfaces and specific trigger mechanisms.

Physiological Role of Phospholipid Exchange through SP-A Contacts. A distinguishing feature of the protein-mediated exchange is that it can be modulated at the contact formation step or at the exchange step (Scheme 1). The calcium-induced change in SP-A promotes its binding to the interface; otherwise, SP-A# self-aggregates. Binding of SP-A# to vesicles is followed by rapid aggregation of vesicles, and the exchange occurs through the SP-A contact between the vesicles. Thus, the locus of action of calcium on SP-A is in the first step, which ultimately determines the partitioning of SP-A# to SP-A* in the interface, or to an unproductive aggregate in the aqueous phase. At this stage we emphasize only the qualitative trends and boundary conditions. However, evolution of a unique model will be facilitated by characterization of calcium- and NaCl-dependent processes, including the state of aggregation of SP-A in the aqueous phase, the nature of the binding equilibrium of SP-A to the vesicle interface, the peptide to vesicle stoichiometry in the aggregation and the exchange steps, and the kinetic stability of the complex that mediates the exchange.

Calcium-triggered selective transfer and exchange of phospholipid by SP-A may have a critical significance for lung function. SP-A appears to be involved in the transfer of phospholipid between the various intracellular compartments under the physiologically relevant conditions. SP-A binds to the saturated phospholipid interface, a distinguishing compositional characteristic of the lung surfactant and the lipid granules of alveolar cells. We suggest that a key role for SP-A is to mediate the exchange of different phospholipid species between the DPPC-rich interfaces. The need for such an exchange will be more acute in situations where unsaturated phospholipids, present as minor components, are (per)-oxidized due to the relatively high partial pressure and exposure to oxygen in the lung. Thus, specific phospholipid in the donor and acceptor interfaces will be equilibrated by SP-A, leading to replenishment at the target interfaces. It is also possible that, coupled with a suitable driving force, SP-A-mediated exchange could result in net transfer of phospholipid, e.g., during the expansion−contraction cycle of the alveolar monolayer. Net transfer of phospholipid from a donor to acceptor membrane could also occur if some of the phospholipid species are removed by a sequential process. Also coupled with a transbilayer movement mechanism, the exchange through contacts could control the composition on the transbilayer side.

To recapitulate, SP-A- and calcium-mediated membrane−membrane contacts capable of selective exchange of phospholipid could be involved in trafficking and sorting of phospholipid between cellular compartments. The mechanism that we envisage here brings about exchange between the outer monolayer of the membranes in contact, without the merger or mixing of distal monolayer, or mixing of aqueous compartments. This permits selective exchange of lipid species between membrane monolayers in contact. Thus, depending on the composition of the monolayers in contact, and the selectivity of the exchange, SP-A contacts could be useful for the removal or replenishment of specific lipid components.

REFERENCES

1. King, R. J., Klass, D. J., Gikas, E. G., and Clements, J. A. (1973) *Am. J. Physiol. 224*, 788−795.
2. Hawgood, S., and Shiffer, K. (1989) *Annu. Rev. Physiol. 53*, 375−394.
3. Kuroki, Y., and Voelker, D. R. (1994) *J. Biol. Chem. 269*, 25943−25946.
4. Voss, T., Eistetter, H., Schafer, K. P., and Engel, J. (1988) *J. Mol. Biol. 201*, 219−227.
5. Spissinger, T., Schaffer, K. P., & Voss, T. (1991) *Eur. J. Biochem. 199*, 65−71.
6. Haagsman, H. P., Sargeant, T., Hauschka, P. V., Benson, B. J., and Hawgood, S. (1990) *Biochemistry 29*, 8894−8900.
7. King, R. J., Phillips, M. C., Horowitz, P. C., and Dang, S. C. (1986) *Biochim. Biophys. Acta 879*, 1−13.
8. Efrati, H., Hawgood, S., Williams, M. C., Hong, K., and Benson, B. J. (1987) *Biochemistry 26*, 7986−7993.
9. Williams, M. C., Hawgood, S., and Hamilton, R. L. (1991) *Am. J. Respir. Cell Mol. Biol. 5*, 41−50.
10. Kuroki, Y., and Akino, T. (1991) *J. Biol. Chem. 266*, 3068−3073.
11. Fisher, A. B., Dodia, C., and Chander, A. (1994) *Am. J. Physiol. 267*, L335−341.
12. Meyboom, A., Maretzki, D., Stevens, P. A., and Hofmann, K. P. (1997) *J. Biol. Chem. 272*, 14600−14605.
13. McCormack, F. X., Stewart, J., Voelker, D. R., and Damodarasamy, M. (1997) *Biochemistry 36*, 13963−13971.
14. Casals, C., Miguel, E., and Perez-Gil, J. (1993) *Biochem. J. 298*, 585−593.
15. Kuroki, Y., McCormack, F. X., Ogasawara, Y., Mason, R. J., and Voelker, D. R. (1994) *J. Biol. Chem. 269*, 29793−29800.
16. Kuroki, Y., Mason, R. J., and Voelker, d. R. (1988) *J. Biol. Chem. 263*, 17596−17602.
17. Suzuki, T. (1989) *Am. Rev. Respir. Dis. 140*, 75−81.
18. Ellens, H., Bentz, J., and Szoka, F. C. (1985) *Biochemistry 24*, 3099−3106.
19. McIntyre, J. C., and Sleight, R. G. (1991) *Biochemistry 30*, 11819−11827.
20. Hoekstra, D., Buist-Arkema, R., Klappe, K., and Reutelingsperger, C. P. M. (1993) *Biochemistry 32*, 14194−14202.
21. Düzgünes, N., and Wilschut, J. (1993) *Methods Enzymol. 220*, 3−14.
22. Hoekstra, D., and Düzgünes, N. (1993) *Methods Enzymol. 220*, 15−31.
23. Cajal, Y., Berg, O. G., and Jain, M. K. (1995) *Biochem. Biophys. Res. Commun. 210*, 746−752.
24. Cajal, Y., Rogers, J., Berg, O. G., and Jain, M. K. (1996) *Biochemistry 35*, 299−308.
25. Cajal, Y., Ghanta, J., Easwaran, K., Surolia, A., and Jain, M. K. (1996) *Biochemistry 35*, 5684−5695.
26. Cajal, Y., and Jain, M. K. (1997) *Biochemistry 36*, 3882−3893.
27. Cajal, Y., Boggs, J. M., and Jain, M. K. (1997) *Biochemistry 36*, 2566−2576.
28. Jain, M. K., and Vaz, W. L. C. (1987) *Biochim. Biophys. Acta 905*, 1−8.
29. Haagwood, S., Benson, B. J., and Hamilton, R. L. (1985) *Biochemistry 24*, 184−190.
30. Bates, S. R., and Fisher, A. B. (1996) *Am. J. Physiol. 271 (Lung Cell. Mol. Physiol. 15)*, L258−266.
31. Hallman, M., Spragg, R., Harrell, J. H., Moser, K. M., and Gluck, L. (1982) *J. Clin. Invest. 70*, 673−683.
32. White, J. M. (1992) *Science 258*, 917−924.

33. Moreau, P., and Cassagne, C. (1994) *Biochim. Biophys. Acta 1197*, 257−290.
34. Rothman, J. E. (1996) *Protein Sci. 5*, 185−194.
35. Hoekstra, D. (1990) *J. Bioenerg. Biomembr. 22*, 121−128.
36. Ferro-Novick, S., and Jahn, R. (1994) *Nature 370*, 191−193.
37. Hughson, F. M. (1995) *Curr. Opin. Struct. Biol. 5*, 507−513.
38. Schweizer, F. E., Betz, H., and Augustine, G. J. (1995) *Neuron 14*, 689−696.
39. Südhof, T. (1995) *Nature 375*, 645−653.
40. Weber, T., Zemelman, B. V., McNew, J. A., Westermann, B., Gmachi, M., Parlati, F., Sollner, T. H., and Rothman, J. E. (1998) *Cell 92*, 759−771.
41. Dawidowicz, E. A. (1987) *Curr. Top. Membr. Transp. 29*, 175−210.
42. Wirtz, K. W. A. (1991) *Annu. Rev. Biochem. 60*, 73−94.
43. Cajal, Y., and Jain, M. K. (1995) *J. NIH Res. 8*, 35−39.

BI980122S